

Optimising of operation conditions for carbon nanotube production using pyrolysis coupled with catalytic chemical vapor deposition

Mohd Syazwan Mohd Ghazali^{1,2}, Mohd Saufi Md Zaini^{3*}, Siti Zaharah Roslan⁴,
Syed Shatir A. Syed-Hassan⁵

¹Section of Environmental Engineering, Universiti Kuala Lumpur, Malaysia Institute of Chemical and Bioengineering, 78000 Alor Gajah, Melaka, Malaysia

^{2,4,5}School of Chemical Engineering, College of Engineering, Universiti Teknologi MARA, 40450 Shah Alam, Selangor, Malaysia

³Chemical Engineering Studies, College of Engineering, Universiti Teknologi MARA Cawangan Terengganu, Kampus Bukit Besi, 23200 Dungun, Terengganu, Malaysia

ARTICLE INFO

Article history:

Received 26 March 2024

Revised 10 September 2024

Accepted 12 September 2024

Online first

Published 31 October 2024

Keywords:

Sewage Sludge

Carbon nanotube

Catalytic chemical vapour
deposition

Response surface methodology

DOI:

10.24191/mjct.v7i2.1254

ABSTRACT

Sewage sludge holds great potential for producing carbon nanotubes (CNTs) due to their abundance, renewability, and low-cost carbon source. The objective of this study is to investigate the production of CNTs through two-stage processes i.e. pyrolysis and catalytic chemical vapor deposition (CCVD) of sewage sludge-derived vapor. The central composite design (CCD) model of response surface methodology (RSM) was conducted to predict and optimise the yield of CNTs from sewage sludge vapour. The statistical results indicate that the optimal conditions are a catalyst loading of 0.5 and a temperature of 800 °C. The catalyst loading has the greatest impact on CNTs yield, as evidenced by the F-value in the ANOVA. The actual CNTs yield under these optimal conditions was 30.53%, which is in close agreement with the predicted value of 33.60%. A quadratic model was employed to investigate the relationship between temperature and catalyst load on the deposition yield of CNTs. The CNTs were then characterised using Raman Spectroscopy, X-ray Diffraction (XRD), Field Emission Scanning Electron Microscope (FESEM) and Transmission Electron Microscopy (TEM). The optimised CNTs had an outer diameter of 25.2 nm, and inner diameters of 3.2 nm. This research contributes to the advancement of the CNTs production from sewage sludge.

^{3*}Corresponding author. E-mail address: saufizaini@uitm.edu.my
<https://doi.org/10.24191/mjct.v7i2.1254>

1. INTRODUCTION

Sewage sludge is a by-product of the wastewater treatment process. It is a carbon-rich material that is difficult to store due to its high-water content and the presence of nitrogen and oxygen-containing compounds (Roslan et al., 2023; Syed-Hassan et al., 2017). Despite these obstacles, sewage sludge holds significant potential as a cost-effective and accessible carbon source, requiring additional conversion for beneficial use. Pyrolysis is a process to convert feedstock into bio-char, bio-oil, and gases (Zaini & Jalil, 2021). Unfortunately, the conventional pyrolysis process of converting sewage sludge into bio-oil does not fully utilize its potential. The resulting energy output is lower than that of conventional fuels, which generally produce around 40 MJ of energy (Arazo et al., 2017; Liu et al., 2020). Instead of settling for an underwhelming outcome like almost useless bio-oil or meagre heat generation (Hsu et al. 2023). Our research focuses on producing carbon nanotubes (CNTs) by combining the catalytic chemical vapour deposition (CCVD) process with pyrolysis. This approach offers a more sustainable and comprehensive solution by directly converting the evolving sewage sludge vapour into valuable CNTs.

CNTs have received considerable attention since they were discovered by Ijima in the 1990s (Prasek et al. 2011; Paul et al. 2023). Their simple chemical composition and atomic bonding configuration (Gupta et al. 2019) contribute to their diverse structures and exceptional mechanical, thermal, and electrical properties (Aboul-enein et al., 2021; Düндar-Tekkaya & Karatepe, 2015). Over the past few decades, efforts to economically produce and maximize the diverse advantages of CNTs for various applications have attracted increased research interest (Zhang et al., 2020). Their versatile properties have found applications in various fields including electronics, energy storage, catalysis, and water treatment (Düндar-Tekkaya & Karatepe, 2015; Hou et al., 2017; Mazumder et al., 2015; Ming et al., 2016). Researchers have explored various techniques for CNTs growth, including arc discharge, laser ablation, CCVD, and temperature-directed synthesis (Dutta et al., 2020). Among these methods, CCVD has emerged as the most practical approach in terms of simplicity, versatility, energy consumption, and cost-effectiveness and has been widely adopted by numerous researchers (Lobiak et al., 2020)

The use of suitable carbon sources for CNT growth is a critical aspect of the CCVD process. Conventional carbon sources such as carbon monoxide (CO), acetylene (C₂H₂), ethylene (C₂H₄), and methane (CH₄) have traditionally been used for CNTs growth (Wang et al., 2020). However, researchers recognize the need for further investigation of the sustainability of these conventional carbon sources. Hence, CCVD studies have been extended to explore unconventional carbon sources such as coal, kerosene, palm oil, green grass, and plastic waste (Aziz et al., 2012; Shah and Tali, 2016). This expanded research enriches our understanding of CNTs synthesis by exploring diverse carbon sources and novel, economical, and sustainable raw materials.

Response surface methodology (RSM) is an optimization tool used to evaluate the significance of multiple factors and their interactions (Jalil et al., 2022). Two studies have demonstrated the application of RSM to optimise CNTs, as reported by Allaedini et al. (2016) and Mohammadian et al. (2018). Both studies examined critical parameters such as catalyst concentration, hydrogen flow rate, and synthesis temperature. Mohammadian et al. (2018) revealed that the optimal CNTs were produced at temperature of 976 °C and a catalyst concentration of 3.78 wt% with a hydrogen flow rate of 184 cm³/min. Moreover, Allaedini et al. (2016) revealed that the prepared catalyst exhibited high crystallinity, a small average particle diameter of 253 nm), and uniform, multi-walled CNTs with a diameter of approximately 18 nm. These CNTs displayed a significant degree of graphitization and remarkable oxidation stability.

The study by Aljumaily et al. (2018) aimed to optimise the carbon yield and contact angle during the synthesis of CNTs from methane by adjusting the reaction temperature, time, and H₂/C₂H₂ gas ratio. The optimal temperature was found to be 702 °C for a carbon yield of 380% and 687 °C for a contact angle of

177 °C. A reaction time of 40 min and a gas ratio of 1.0 had a significant impact on both the yield and angle. Furthermore, Boufades et al. (2022) optimised the production of hydrocarbon-based CNTs by fine-tuning the time, temperature, and catalyst-to-condensate gas mass ratio. This optimization resulted in a predicted yield of 81.76% under optimal conditions, which included a reaction temperature of 1000 °C, reaction time of 112 min, and catalyst-to-condensate gas weight ratio of 5%. These findings closely aligned with the experimental value of 80.81%.

Given the potential for modest production of CNTs from sewage sludge-derived vapour in this study, it is particularly important to explore the potential of employing RSM as a technique to optimise the desired outcome. Finding the right process variables in a two-stage coupling process is a complex challenge that demands a careful balance between these variables. The growth factors or variables, such as carbon source, catalyst, and substrate, significantly influence the final carbon product in the CCVD (Manawi et al., 2018). Temperature is the most significant factor, typically ranging from 500 to 1000°C (Kumar & Ando, 2010). Considerably, the catalyst emerges as another crucial parameter in capturing complex precursors derived from sewage sludge, utilizing nanoparticle catalysts for deposition and substrates as support materials (Shah & Tali, 2016). The amount of catalyst used has a direct impact on CNTs formation, with iron, cobalt, and nickel being prominent metal catalysts (Makgabutlane et al., 2021).

This study aims to optimise parameters such as reaction temperature and catalyst loading to maximize CNTs yield using RSM. The process involves two stages to produce CNTs from sewage sludge. In the first stage, slow pyrolysis decomposes the sewage sludge into organic vapor, which then flows into a CCVD reactor where nano-sized carbon material grows on the catalyst substrate. This approach enhances the efficiency of CNTs production while also supporting sustainable waste management by repurposing sewage sludge as a valuable resource. The impact of the critical parameters on the growth of CNTs was examined in this study. The CNTs were thoroughly analysed using advanced techniques, including X-ray diffraction (XRD), Raman spectroscopy, field emission scanning electron microscopy (FESEM), and high-resolution transmission electron microscopy (TEM), which provided valuable information about the structure and properties of the CNTs. These results are crucial for determining the effects of these essential parameters on the CNTs growth.

2. METHODOLOGY

2.1 Material and catalyst preparation

In this study, sewage sludge was obtained from a sewage treatment plant in Sungai Udang, Melaka. The sewage sludge was dried in an oven at 105 °C for 24 h (Ping & Wang, 2016). The dried sewage sludge was then stored in an airtight container for prior analysis. For catalyst preparation, 3 g of cobalt (II) nitrate hexahydrate ($\text{Co}(\text{NO}_3)_2 \cdot 6\text{H}_2\text{O}$, 99.99% trace metals basis, Sigma Aldrich, Germany) was mixed and dissolved in 2 ml of ethanol ($\text{CH}_3\text{CH}_2\text{OH}$, 99.5%, Merck, Germany). Then, 3 g of aluminium oxide (Al_2O_3 , Sigma Aldrich, Germany) was added to the mixture as a catalyst support and stirred until a slurry was formed. The mixture was dried overnight in an oven at 50 °C to remove residual ethanol. Subsequently, the dried slurry was calcined in a muffle furnace at 1000 °C for 3 h to completely convert and stabilize the material.

2.2 Physicochemical characteristics of the sewage sludge

For proximate analysis on a dry basis, the sample underwent combustion at 950 °C for 3 h in accordance with ASTM D3174, to determine the ash content (A). The volatile matter content (VM) was calculated by measuring the weight loss after 7 min at 950 °C following the method specified in ASTM E872-82.

The fixed carbon content (FC) was calculated from this difference. The elemental compositions of C, H, N, and S were determined using a Vario EL III elemental analyser for ultimate analysis. The O content was determined by subtracting the combined weight percentage of all the elements and ash from 100%.

2.3 Experimental set-up and procedure

The experimental setup utilized in this study is shown in Fig. 1, which illustrates a configuration comprising two distinct types of reactors. The first reactor, made of stainless steel, had an inner diameter of 50 mm and a height of 155 mm and served as a pyrolysis reactor. The second reactor, also fabricated from stainless steel, was a CCVD reactor 35 mm in diameter and 350 mm in length. Both reactors were carefully positioned within the electric furnaces to ensure controlled heating. The procedure involved a two-stage coupling technique, including pyrolysis, followed by CCVD. In the first stage, sewage sludge is deposited in the initial reactor (pyrolysis). This setup entailed connecting the exit of the first-stage reactor with the second-stage reactor through pyrolysis-CCVD coupling to synthesize CNTs. This configuration facilitated the implementation of the CCVD process for the vapour generated within the pyrolysis reactor. Subsequently, it couples with the second reactor (CCVD reactor), which houses the catalyst for the growth of CNTs.

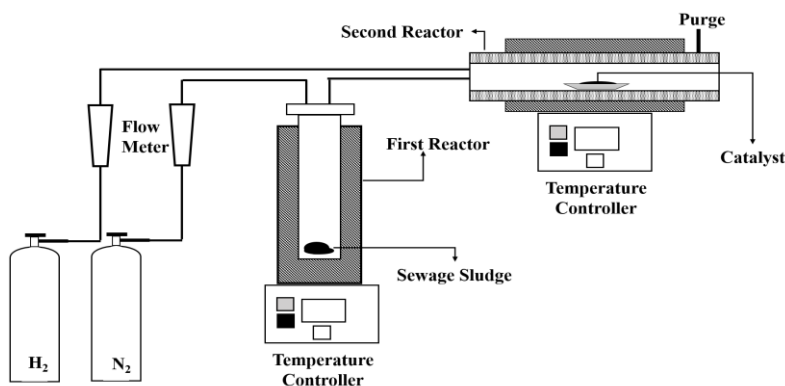


Fig. 1. A schematic diagram of the two-stage coupling process: pyrolysis-CCVD process

Source: Author's own illustration

2.4 Production of CNTs

The process involved the use of an alumina combustion boat measuring 90 mm × 17 mm × 11.5 mm, which was loaded with varying amounts of cobalt catalyst (0.2 - 0.8 g) that had been reduced with hydrogen gas at rate of 0.5 L/min. The temperature of the second reactor was increased to various temperatures as indicated in Table 1. 10 g of sewage sludge was loaded into the first reactor, which was purged with a continuous flow of nitrogen gas at a rate of 0.5 L/min and maintained at a pyrolysis temperature of 550 °C for 30 min. The final weight of carbon deposited on the catalyst was recorded to determine the yield of CNTs (%) using Equation (1) (Hussein et al. 2014).

$$\text{yield} = \frac{\text{weight of carbon deposited (mg)}}{\text{initial weight of metal oxide}} \times 100\% \quad (1)$$

2.5 Optimisation of CNTs production

The CNTs were optimised based on the highest yield achieved using the pyrolysis-CCVD approach. A response surface methodology (RSM), employing a central composite design (CCD), was used to optimise the CCVD synthesis temperature (A), which ranged from 730 to 870 °C, and catalyst load (B), which varied between 0.2 g and 0.8 g. Table 1 lists the experimental parameters and ranges used in the CCD.

A rotatable CCD design matrix was selected, comprising five factorial points, four axial points, and four replicates at the center points, resulting in 13 experiments (Table 2). To analyse the experimental data, Design Expert 11.1.2.0 (STAT-EASE Inc., Minneapolis, USA) was utilised, which involved conducting analysis of variance (ANOVA) and regression analysis to develop the necessary equations. The total number of runs was determined using Equation (2), and a second-order polynomial of Equation (3) was employed to investigate the interaction between the parameters and response behaviour.

$$N = 2^k + 2k + C_o = 2^2 + 2 * 2 + 5 = 13 \quad (2)$$

$$Y = \beta_o + \sum_{i=1}^k \beta_i x_i + \sum_{i=1}^k \beta_i x_i^2 + \sum_{i=j}^k \sum_{i=1}^k \beta_{ij} x_i x_j \quad (3)$$

Table 1. Summary of the experimental design for CNTs yield

Factor	Name	Units	Type	Min	Max	Coded Low	Coded High	Mean	Std. Dev.
A	Temperature	°C	Numeric	730	870	-1 ↔ 730.00	+1 ↔ 870.00	800	40.62
B	Catalyst	g	Numeric	0.2	0.8	-1 ↔ 0.20	+1 ↔ 0.80	0.6	0.16

Source: Author's own data

Table 2. Experimental design matrix and results

Run	Factor 1 A: Temperature (°C)	Factor 2 B: Catalyst (g)
1	800	0.2
2	730	0.5
3	800	0.5
4	800	0.5
5	800	0.5
6	800	0.5
7	750	0.3
8	870	0.5
9	750	0.7
10	850	0.7
11	800	0.8
12	850	0.3
13	800	0.5

Source: Author's own data

2.6 Characterisation of CNTs

The carbon deposited on the cobalt catalyst in the CCVD reactor was analysed to determine the presence of CNTs and characterise their properties. X-ray diffraction patterns of the carbon materials were obtained, and the crystal structure was analysed using an X-ray diffractometer (PANalytical X'pert Pro diffractometer) coupled with Cu K radiation ($\lambda = 0.154$ nm) within the measuring range of 2θ of 0° to 10° . The synthesis of CNTs was validated using a Raman spectrophotometer (UniRAM-500, UniRAM, South Korea) with an excitation wavelength of 532 nm. Finally, the surface morphology and diameter of the CNTs were examined using a JEOL JSM 7600F field emission scanning electron microscopy (FE-SEM) and JEOL JEM-2100F transmission electron microscopy (TEM).

3. RESULT AND DISCUSSION

3.1 Physicochemical Properties of the Sewage Sludge

Table 3 presents the results of proximate and ultimate analyses of a dried sample of sewage sludge. The results indicate a considerable amount of organic matter in the sludge, notably with a carbon content of 24.7% and volatile matter content of 37%. Sewage sludge is a promising carbon source due to its high VM content, which is essential for CNTs formation and serves as a potential precursor in the process. The high percentages of nitrogen (7.1%) and sulfur (0.9%) are consistent with previous studies, as these elements are derived from the decomposition of protein components by microbes during the water treatment process (Naqvi et al., 2019). These characteristics provide a basis for the synthesis of CNTs from sewage sludge using a two-stage coupling process.

Table 3. Ultimate and proximate analysis of sample

Sample	Sewage Sludge ^a	
Ultimate analysis (wt. %)	C	24.7
	H	2.7
	N	7.1
	S	0.9
	O ^b	17.3
Proximate Analysis (wt. %)	FC ^c	15.7
	VM	37.0
	Ash	47.3

^a Dry basis

^b Determined by difference.

^c $FC = 100 - (Ash + VM)$

Source: Author's own data

3.2 Production of CNTs via two-stage coupling process

In this study, the sewage sludge, in the form of pyrolysis-derived vapor, becomes a fixed growth factor in the CCVD process. Correspondingly, carbon deposition occurred in the temperature range of 730 to 870 °C, caused by gaseous hydrocarbons adsorbed and dissociated on the surface of the catalyst particles. This process leads to the formation of basic carbon atoms that precipitate and crystallize (Zhang et al., 2021). Table 4 summarises the results of the 13 tests performed in this study, detailing the carbon deposition yields at different temperatures and catalyst loadings. The results indicate a close alignment between the

predicted and actual values for the yield of CNTs produced, demonstrating the reliability and effectiveness of the predictive model employed. The actual carbon deposition yield values range from 10.2% to 33.6%.

The findings show a non-linear relationship between temperature and deposition yield, with yield decreasing as the temperature increased. This result is comparable with that of a study by Li et al. (2002), who found that a temperature of 800 °C yielded maximum deposition. At this temperature, the high catalytic activity of cobalt and vapour decomposition are optimally combined, resulting in maximum deposition and enhanced contact between the catalyst and carbon atoms. Simultaneously, the vapours break down the carbon-containing component into carbon and other species and the metal catalyst nanoparticles are further activated, allowing the maximum dissolution of carbon into the metal. Consequently, the dissolved carbon forms a cylindrical network with no dangling bonds, making it energetically stable after reaching the carbon solubility limit in the metal at that temperature (Henao et al., 2021). As the temperature increased, the deposition yields significantly decreased, exhibiting degradation that occurred simultaneously owing to an inverse contact between the temperature and catalyst.

Table 4. Actual and predicted values of yield CNTs

Run Order	Actual, %	Predicted, %
1	22.50	22.97
2	10.20	10.43
3	28.30	30.32
4	30.00	30.32
5	30.20	30.32
6	29.70	30.32
7	18.30	17.40
8	17.30	14.97
9	12.20	13.37
10	14.50	17.46
11	20.50	18.20
12	18.90	19.79
13	22.50	22.97

Source: Author's own data

Fig. 2 shows a visual representation of the predicted values plotted against the experimental values of the CNTs yield. Overall, the yield of the CNTs was comparable to that predicted by the experimental design (DOE). The remarkable similarity between these values indicates strong agreement, highlighting the effectiveness of the developed model in accurately representing the correlation between the CNTs yields and the selected variable

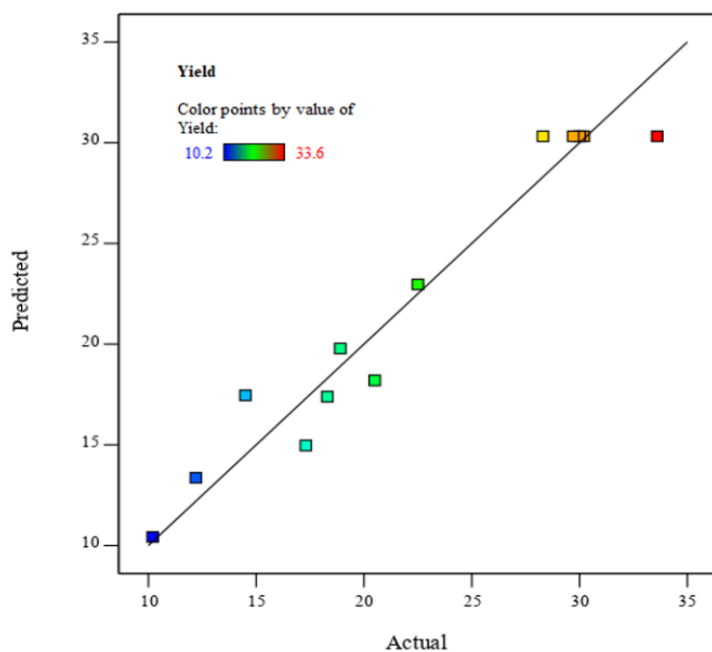


Fig. 2. Predicted vs. actual yield of CNTs

Source: Author's own data

3.3 Statistical model analysis

Table 5 shows the analysis of variance (ANOVA) for the selected model for the CNT yield. The results unequivocally support the adequacy of the predicted model for deposition yield. The obtained regression model exhibited a high level of significance ($P < 0.05$), with an R^2 value of 0.9459 and an adjusted R^2 of 0.9073. A higher R^2 value indicates better model performance, reflecting the proximity of the predicted values to the actual response values (Shahbeig & Nosrati, 2020). Furthermore, the predicted R^2 value of 0.7345 demonstrated reasonable agreement with the adjusted R^2 value of 0.9073, with a difference of less than 0.2. While the model performs well with the current data, the discrepancy suggests it may have limitations in predicting conditions with different temperatures or catalyst loadings.

The insignificance of the lack-of-fit F-value suggests a satisfactory agreement between the experimental and predicted values, validating the suitability of the proposed quadratic model for the investigation. The F-value of 24.5 and p-value of 0.0003 emphasize the significance of the developed model, indicating that the terms included in the model are statistically significant. Although individual factors (temperature, catalyst, and their interaction) were not significant, the discrepancy in the P value was not too large. This might be due to several errors made during the experiment such as human error or analytical error. Nevertheless, the overall model remains valid.

According to Kirby (2006), an F-value greater than four indicates a significant effect of control factors on the response. Therefore, it can be concluded that the catalyst is the most influential factor in this study, with an F-value of approximately 4.

Table 5. Analysis of variance (ANOVA) for quadratic model for yield of CNTs

Source	Sum of Squares	df	Mean Square	F-value	p-value	
Model	666.13	5	133.23	24.5	0.0003	significant
A-Temperature	20.82	1	20.82	3.83	0.0913	
B-Catalyst	21.44	1	21.44	3.94	0.0874	
AB	0.7225	1	0.7225	0.1329	0.7262	
A ²	541.3	1	541.3	99.55	< 0.0001	
B ²	156.66	1	156.66	28.81	0.001	
Residual	38.06	7	5.44			
Lack of Fit	22.73	3	7.58	1.98	0.2596	not significant
Pure Error	15.33	4	3.83			
Cor Total	704.2	12				
R ²	0.9459					
Adjusted R ²	0.9073					
Predicted R ²	0.7345					
Standard Deviation	2.33					

Source: Author's own data

3.4 Development of regression model equation

Based on the analysis of the sequential model sum of squares, selecting the highest-order polynomials allowed for the identification of a suitable model that exhibited significant additional terms and avoided aliasing. In this regard, a quadratic model emerged as the recommended choice, effectively capturing the intricate relationship between the temperature (A) and catalyst load (B). The derived coded equation, expressed in Equation (4), concisely shows the following relationship.

$$\text{Yield of CNTs} = 30.32 + 1.62 A - 1.59 B + 0.4250 AB - 8.99 A^2 - 4.33 B^2 \quad (4)$$

In general, the positive signs of the coefficients within the model signify a synergistic effect on the deposition process, indicating a cooperative relationship between the variables. Conversely, the negative signs of the coefficients suggest antagonistic effects, implying a counteractive influence between factors. Notably, the developed model revealed the crucial role of temperature in governing the deposition process, underscoring its significance concerning the precursor and catalyst.

3.5 Effect of operating variables on CNTs yield

Fig. 3 illustrates the perturbation plot at 800 °C and 0.5 g, as well as the interaction plot of variables A and B. The red line indicates the catalyst loading which is 0.7 g, whereas the black line indicates the catalyst loading of 0.3 g.

In the perturbation plot (Fig. 3 (a)), B shows a sensible effect, slightly stronger than A based on the F-value, indicating that the catalyst has a somewhat greater influence on the yield. However, the catalyst primarily affects the yield by shifting it upwards or downwards rather than altering the shape of the response. On the other hand, the significant curvature of the temperature's effect is captured by the quadratic term, A². This highlights a non-linear relationship, indicating an optimal temperature for maximizing yield.

At 750 °C, the shift in CNTs yield was minimal when the catalyst loading was varied from high to low (red line to black line). However, at higher temperatures, the yield shift became more pronounced (see Fig. 3(b)). Based on the figure, the most notable changes in yield occur near 800 °C with a catalyst loading of 0.5 g. Then, the yield drops sharply after the temperature exceeds 830 °C.

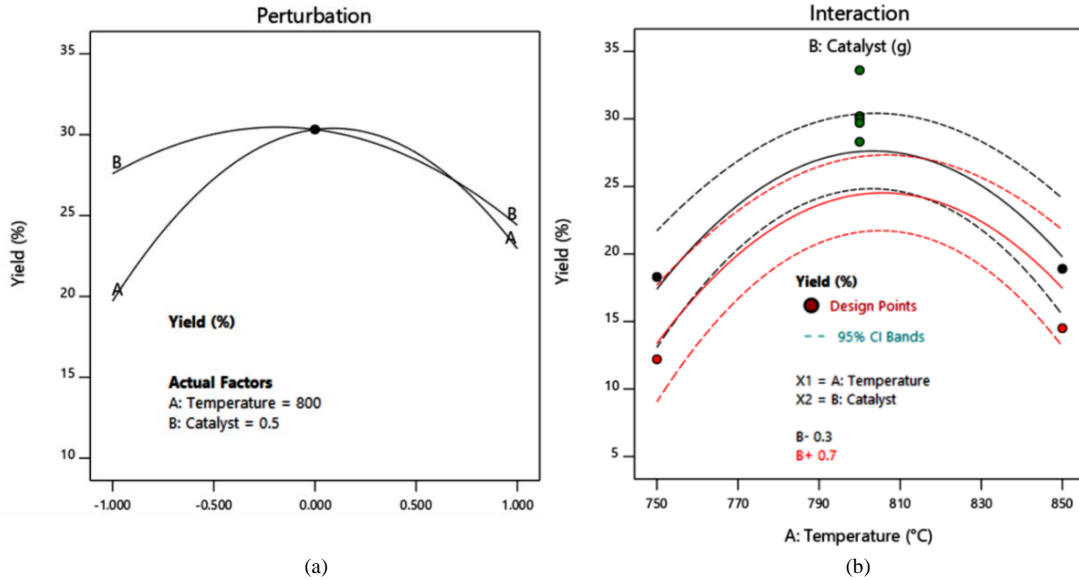


Fig. 3. (a) Perturbation plot on yield at point A = 800°C and B = 0.5 g; (b) Interaction plot between factor A and B; red line catalyst loading at 0.7 g, black line catalyst loading at 0.3 g

Source: Author's own data

The obtained regression model highlights the influence of synthesis temperature and catalyst loading on CNTs production. Acting as a crucial template or nucleation site, the catalyst film in CCVD facilitates the growth of the desired material, as described by Henao et al., (2021). Moreover, under elevated temperature conditions, the interaction between hydrocarbon vapours and metal nanoparticles was enhanced, facilitating the effective dissolution of carbon into the metal (Zhang et al., 2021). The highest CNTs yield is achieved with catalyst loadings between approximately 0.4 and 0.6 g. In this case, there might be a saturation point where the excess catalyst does not significantly contribute to the catalytic activity or may even lead to issues such as catalyst aggregation or deactivation (Yu et al., 2005). Therefore, keeping the catalyst loading within this optimal range is important to ensure it remains an effective template.

The convex three-dimensional surfaces (Fig. 4(a)) and contour plot graphs (Fig. 4(b)) indicate the quadratic effects of temperature, A and catalyst, B on CNTs yield. The elliptical shape results from the second-order polynomial model, as shown in Equation (4). The most significant factor influencing yield was A^2 . An increase in temperature led to a decrease in carbon deposition, which was directly linked to catalyst deactivation at high temperatures and a subsequent decline in the carbon yield. It is noted that as the temperature increased beyond 800 °C, the CNTs yield decreased. This reduction in carbon yield may be due to catalyst deactivation and changes in the precursor vapor species. The capabilities of catalysts as templates for CNTs growth decline due to thermal sintering, which leads to a loss of catalytic activity and impedes carbon atom absorption (Lim et al., 2023). Additionally, some easily decomposable carbon-containing molecules may transform into more stable species, which can slow down carbon growth (Mohd Ghazali et al., 2024).

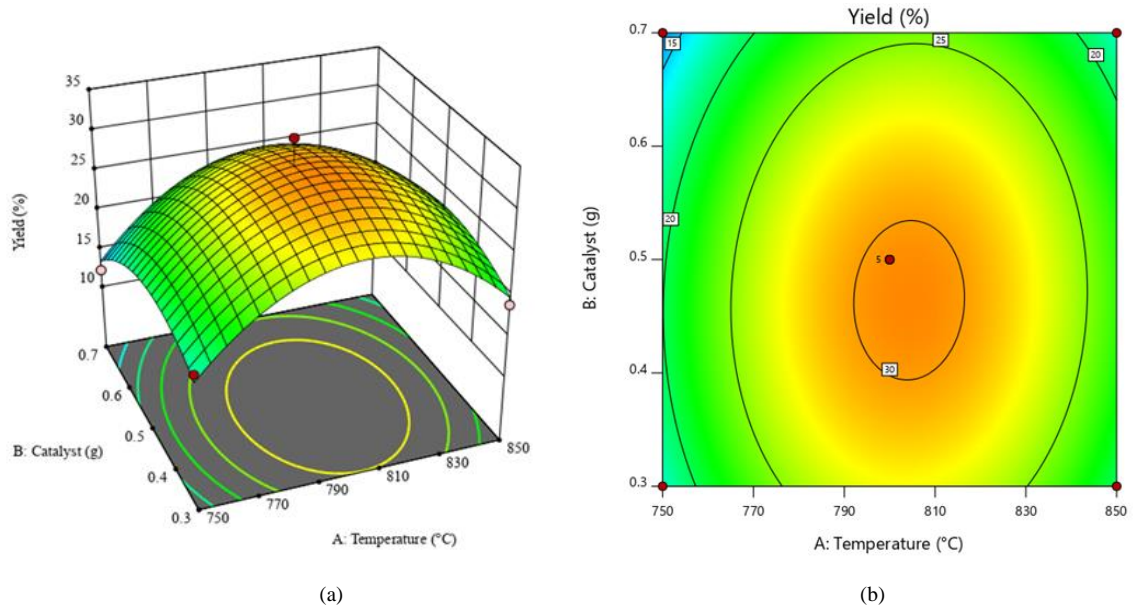


Fig. 4. (a) Three-dimensional (3D) response surface plot illustrating the interaction between temperature and catalyst loading on the response yield; (b) contour plot depicting the variation in response yield with changes in temperature and catalyst

3.6 Process optimisation

The findings in Fig. 5 and Table 6 demonstrate the optimal operating conditions for CCVD, with a temperature of 800 °C (± 5 °C) and a catalyst load of 0.5 (± 0.05) g. The results indicate that the predicted model yielded optimal CNTs with a yield of 30.53%. After conducting experiments under the optimal conditions, the actual yield of CNTs was determined to be 33.6%. The results showed that the predicted data from the models were close to the experimental data, with a 9.14% error, providing compelling evidence for an optimal point in the CCVD process.

Table 6. Validation of optimum conditions for CNTs yield

Temperature (°C)	Catalyst (g)	Yield (%)		Error (%)	Temperature (°C)	Catalyst (g)
		Predicted	Experimental			
800 (± 5)	0.5 (± 0.05)	30.53	33.6	9.14	800 (± 5)	0.5 (± 0.05)

Source: Author's own data

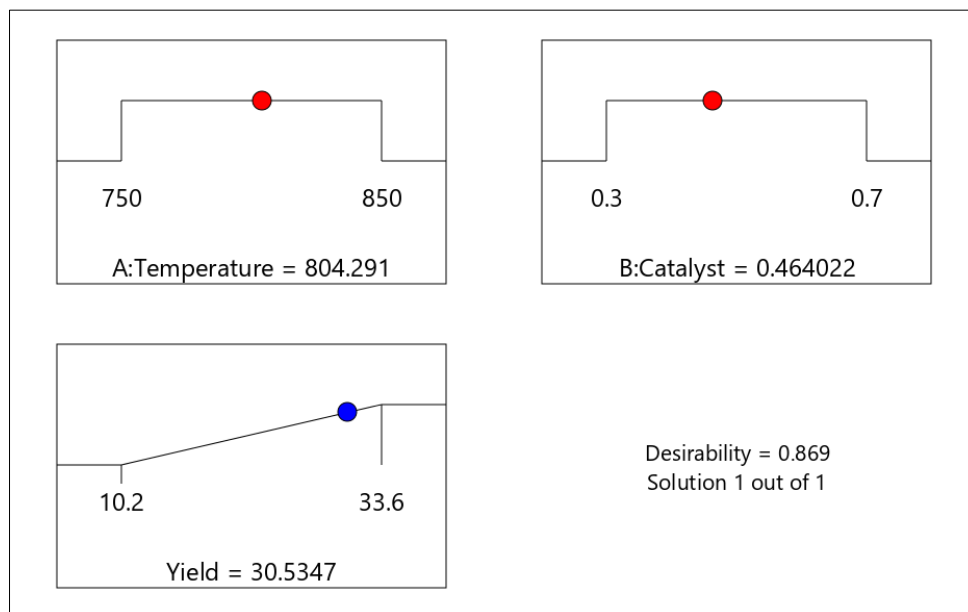


Fig. 5. Recommended condition for optimisation process

Source: Author's own data

3.7 Characterisation of carbon nanotubes

The characterisation of CNTs under the optimum conditions of 800°C and 0.5 g of catalyst loading was further discussed in this section, including XRD, Raman spectroscopy, FESEM, and TEM analyses.

3.7.1 X-ray diffraction

Fig. 6 shows the XRD patterns produced by the carbon deposition process. The pattern exhibits prominent peaks corresponding to metal oxides, such as cobalt oxide (CoO) and aluminium oxide (Al₂O₃), which act as the catalyst and support in the process. The analysis revealed strong peaks at approximately 31°, 35°, and 52°, which corresponded to CoO, confirming its existence. In addition, the peaks at 37°, 43°, and 66° were attributed to Al₂O₃. Notably, there was a distinct peak at 26°, indicating the presence of a graphitic material. The other peaks are low-intensity reflections, as indicated by their Miller indices (h k l) (Das et al., 2014). The presence of CNTs is supported by the observation of a diffraction peak at the (002) plane, which corresponds to the reflection plane of graphite (Hussein et al., 2014; Ming et al., 2016). Therefore, the XRD data demonstrate the high possibility of carbon nanotubes in the obtained deposition.

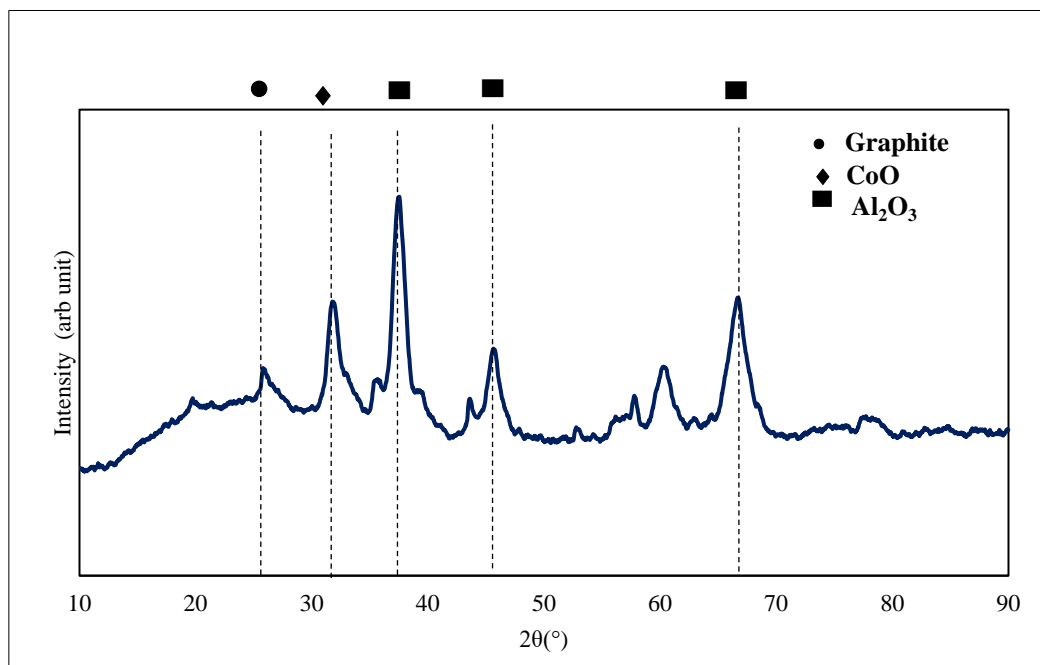


Fig. 6. XRD pattern obtained from the carbon deposition at optimum condition

Source: Author's own data

3.7.2 Raman spectroscopy

Fig. 7 shows the Raman spectrum of the CNTs sample produced under optimal conditions. Researchers widely employ Raman spectroscopy as a valuable tool to assess defects and monitor the quality, crystallinity, and purity of CNTs (Aboul-enein et al., 2021; Lv et al., 2020). The results revealed the presence of CNTs in the synthesized material, and two peaks were detected at approximately 1300 cm^{-1} and 1500 cm^{-1} , corresponding to the D and G bands, respectively. The G-band indicates the graphitization characteristics of the CNTs (Wang et al. 2018), while the D-band peak demonstrates a significant sensitivity towards disordered structures in carbon materials (Ahmad & Silva, 2020). Thus, Raman analysis supports and complements the findings of the XRD analysis, even validating the type of CNTs obtained. The obtained results clearly do not correspond to single-walled carbon nanotubes (SWCNTs) and are more oriented towards multiwalled carbon nanotubes (MWCNTs).

The observed I_D/I_G ratio was 0.99, which provides important insights into its structural characteristics, including the number of defects found on the side walls of the CNTs. This shows that the D band is stronger than the G band, indicating a strong connection with defects (Bîru & Iovu, 2018). This is because the D band reflects carbon atom vibrations, indicating the presence of structure defects in the graphitic layer of CNTs (Aboul-enein et al., 2021).

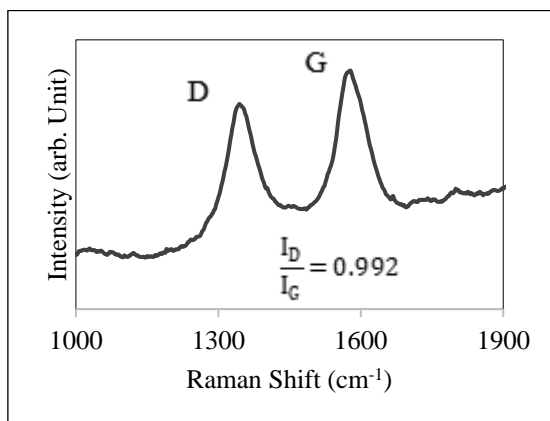


Fig. 7. Raman spectra of CNTs synthesized at optimum yield at 800°C and 0.5 g of catalyst loading

Source: Author's own data

3.7.3 Surface morphology

Fig. 8 shows the surface morphology and dimension of the synthesised CNTs under optimal conditions of 800 °C and 0.5 g catalyst loading. These findings were confirmed by SEM and TEM. The images indicate that the synthesised CNTs had an outer diameter of 25.2 nm, with inner diameters of 3.2 nm. Notably, the images revealed a non-uniform arrangement of the tube walls, indicating the presence of turbostratic features in the CNTs (Belonogov et al., 2021). This observation is consistent with the results obtained from the Raman analysis with respect to the ID/IG ratios, providing further evidence of the relationship between graphitization defects and CNTs characteristics. It is important to note that volatile organics in the precursors have the potential to alter the morphology and graphitization defects of CNTs, which typically consist of cyclic and unsaturated structures. This result is comparable to those of previous studies that successfully produced MWCNTs using unsaturated hydrocarbons (Abdullah et al., 2017; Hernadi et al., 2000).

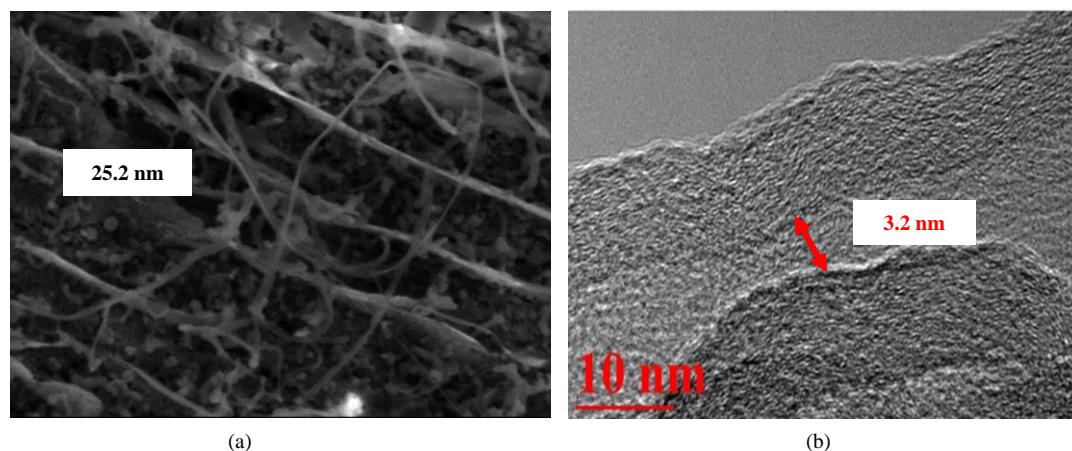


Fig. 8. The structural images (a) SEM (magnification: 100K) and (b) TEM of CNTs under optimal conditions of 800°C and 0.5 g catalyst loading

Source: Author's own data

<https://doi.org/10.24191/mjceet.v7i2.1254>

4. CONCLUSION

The study was conducted to optimise the process parameters for the production of CNTs through a two-stage coupling process involving pyrolysis and CCVD. The study utilised RSM was used to optimise the CCVD process parameters, specifically the reaction temperature and catalyst loading. The optimised conditions, with a temperature of 800 °C and catalyst loading of 0.5 g, resulted in a maximum yield of 30.53%, which was in close agreement with the predicted yield of 33.6%. The quadratic model exhibited a strong correlation between the temperature and catalyst loading on the CNTs yield. The results indicate a non-linear relationship between the synthesis temperature and the yield of CNTs, with the catalyst has a marginally greater influence compared to temperature. The characterisation of the synthesised CNTs using X-ray diffraction, Raman spectroscopy, and transmission electron microscopy confirmed their presence and provided insights into their structural attributes. The obtained CNTs had an outer diameter of 25.2 nm, with an inner diameter of 3.2 nm. Overall, this study enhances the understanding of optimal operational variables and their impacts on processes, particularly on the production of CNTs from sewage sludge through a two-stage coupling process involving pyrolysis and CCVD.

ACKNOWLEDGEMENTS

This project was supported by the Fundamental Research Grant Scheme (FRGS/1/2022/TK0/UITM/02/82). We would like to thank Universiti Teknologi MARA and Universiti Kuala Lumpur for their valuable support during this research project.

CONFLICT OF INTEREST STATEMENT

The authors agree that this research was conducted in the absence of any self-benefits, commercial or financial conflicts and declare the absence of conflicting interests with the funders.

AUTHORS' CONTRIBUTIONS

Mohd Syazwan Mohd Ghazali: Investigation, formal analysis, visualization, writing – original draft. **Mohd Saufi Md Zaini:** validation, writing – review & editing. **Siti Zaharah Roslan:** methodology, validation. **Syed Shatir A. Syed-Hassan:** Conceptualization, funding acquisition, methodology, supervision, project administration, writing – review & editing.

REFERENCES

- Abdullah, H. B., Ramli, I., Ismail, I., & Yusof, N. A. (2017). Hydrocarbon sources for the carbon nanotubes production by chemical vapour deposition: A review. *Pertanika Journal of Science and Technology*, 25(2), 379–396.
- Aboul-Enein, A. A., Arafa, E. I., Abdel-Azim, S. M., & Awadallah, A. E. (2021). Synthesis of multiwalled carbon nanotubes from polyethylene waste to enhance the rheological behavior of lubricating grease. *Fullerenes Nanotubes and Carbon Nanostructures*, 29(1), 46–57. <https://doi.org/10.1080/1536383X.2020.1806828>

- Aboul-enein, A. A., Awadallah, A. E., El-desouki, D. S., & Aboul-gheit, N. A. k. (2021). Catalytic pyrolysis of sugarcane bagasse by zeolite catalyst for the production of multi-walled carbon nanotubes. *Ranliao Huaxue Xuebao/Journal of Fuel Chemistry and Technology*, 49(10), 1421–1434. [https://doi.org/10.1016/S1872-5813\(21\)60127-5](https://doi.org/10.1016/S1872-5813(21)60127-5)
- Ahmad, M., & Silva, S. R. P. (2020). Low temperature growth of carbon nanotubes – A review. *Carbon*, 158, 24–44. <https://doi.org/10.1016/j.carbon.2019.11.061>
- Aljumaily, M. M., Alsaadi, M. A., Das, R., Abd Hamid, S. B., Hashim, N. A., AlOmar, M. K., Alayan, H. M., Novikov, M., Alsahy, Q. F., & Hashim, M. A. (2018). Optimization of the synthesis of superhydrophobic carbon nanomaterials by chemical vapor deposition. *Scientific Reports*, 8(1), 1–12. <https://doi.org/10.1038/s41598-018-21051-3>
- Allaedini, G., Aminayi, P., & Tasirin, S. M. (2016). Methane decomposition for carbon nanotube production: Optimization of the reaction parameters using response surface methodology. *Chemical Engineering Research and Design*, 112, 163–174. <https://doi.org/10.1016/j.cherd.2016.06.010>
- Arazo, R. O., Genuino, D. A. D., de Luna, M. D. G., & Capareda, S. C. (2017). Bio-oil production from dry sewage sludge by fast pyrolysis in an electrically-heated fluidized bed reactor. *Sustainable Environment Research*, 27(1), 7–14. <https://doi.org/10.1016/j.serj.2016.11.010>
- Aziz, A., Maryam, M., & Shamsudin, M. S. (2012). CVD growth of carbon nanotubes from palm oil precursor. May 2014. <https://doi.org/10.1109/ISBEIA.2012.6422908>
- Belonogov, E. K., Kushev, S. B., Soldatenko, S. A., & Turaeva, T. L. (2021). Morphology and structure characteristics of nanoscale carbon materials containing graphene. *Journal of Advanced Materials and Technologies*, 6(4), 247–255. <https://doi.org/10.17277/jamt.2021.04.pp.247-255>
- Bîru, E. I., & Iovu, H. (2018). Graphene nanocomposites studied by Raman spectroscopy. *Raman Spectroscopy*, 9, 179. <https://doi.org/10.5772/intechopen.73487>
- Boufades, D., Hammadou Née Mesdour, S., Moussiden, A., Benmebrouka, H., Ghouti, M., & Kaddour, O. (2022). Optimization of carbon nanotubes synthesis via pyrolysis over Ni/Al₂O₃ using response surface methodology. *Fullerenes Nanotubes and Carbon Nanostructures*, 30(4), 467–475. <https://doi.org/10.1080/1536383X.2021.1956475>
- Das, R., Hamid, S., Ali, M., Ramakrishna, S., & Yongzhi, W. (2014). Carbon Nanotubes Characterization by X-ray Powder Diffraction – A Review. *Current Nanoscience*, 11(1), 23–35. <https://doi.org/10.2174/1573413710666140818210043>
- Dündar-Tekkaya, E., & Karatepe, N. (2015). Investigation of the Effect of Reaction Time, Weight Ratio, and Type of Catalyst on the Yield of Multi-Wall Carbon Nanotubes via Chemical Vapor Deposition of Acetylene. *Fullerenes Nanotubes and Carbon Nanostructures*, 23(10), 853–859. <https://doi.org/10.1080/1536383X.2015.1010641>
- Dutta, S. D., Patel, D. K., & Lim, K. (2020). Chapter 21 - Carbon nanotube-based nanohybrids for agricultural and biological applications. In *Multifunctional Hybrid Nanomaterials for Sustainable Agri-food and Ecosystems*. Elsevier Inc. <https://doi.org/10.1016/B978-0-12-821354-4.00021-2>
- Gupta, N., Gupta, S. M., & Sharma, S. K. (2019). Carbon nanotubes: synthesis, properties and engineering applications. *Carbon Letters*, June 2020. <https://doi.org/10.1007/s42823-019-00068-2>
- Henaó, W., Cazaña, F., Tarifa, P., Romeo, E., Latorre, N., Sebastian, V., Delgado, J. J., & Monzón, A. (2021). Selective synthesis of carbon nanotubes by catalytic decomposition of methane using Co-Cu/cellulose derived carbon catalysts: A comprehensive kinetic study. *Chemical Engineering Journal*, 404, 126103. <https://doi.org/10.1016/j.cej.2020.126103>

- Hernadi, K., Fonseca, A., Nagy, J. B., Siska, A., & Kiricsi, I. (2000). Production of nanotubes by the catalytic decomposition of different carbon-containing compounds. *Applied Catalysis A: General*, 199(2), 245–255. [https://doi.org/10.1016/S0926-860X\(99\)00561-X](https://doi.org/10.1016/S0926-860X(99)00561-X)
- Hou, P. X., Du, J., Liu, C., Ren, W., Kauppinen, E. I., & Cheng, H. M. (2017). Applications of carbon nanotubes and graphene produced by chemical vapor deposition. *MRS Bulletin*, 42(11), 825–831. <https://doi.org/10.1557/mrs.2017.238>
- Hsu, C. Y., Rheima, A. M., Mohammed, M. S., Kadhim, M. M., Mohammed, S. H., Abbas, F. H., Abed, Z. T., Mahdi, Z. M., Abbas, Z. S., Hachim, S. K., Ali, F. K., Mahmoud, Z. H., & Kianfar, E. (2023). Application of Carbon Nanotubes and Graphene-Based Nanoadsorbents in Water Treatment. *BioNanoScience*. <https://doi.org/10.1007/s12668-023-01175-1>
- Hussein, M. Z., Jaafar, A. M., & Yahaya, A. H. (2014). Formation and Yield of Multi-Walled Carbon Nanotubes Synthesized via Chemical Vapour Deposition Routes Using Different Metal-Based Catalysts of FeCoNiAl, CoNiAl and FeNiAl-LDH. *International Journal of Molecular Sciences*, 15(11), 20254–20265. <https://doi.org/10.3390/ijms151120254>
- Jalil, M. J., Rasnan, N. H. A., Yamin, A. F. M., Zaini, M. S. M., Morad, N., Azmi, I. S., Mahadi, M. B., & Yeop, M. Z. (2022). Optimization of Epoxidation Palm-Based Oleic Acid To Produce Polyols. *Chemistry and Chemical Technology*, 16(1), 66–73. <https://doi.org/10.23939/chcht16.01.066>
- Kirby, E. D. (2006). A parameter design study in a turning operation using the Taguchi method. The technology interface, 1-14.
- Kumar, M., & Ando, Y. (2010). Chemical Vapor Deposition of Carbon Nanotubes: A Review on Growth Mechanism and Mass Production. *Journal of Nanoscience and Nanotechnology*, 10(6), 3739–3758. <https://doi.org/10.1166/jnn.2010.2939>
- Li, W. Z., Wen, J. G., & Ren, Z. F. (2002). Effect of temperature on growth and structure of carbon nanotubes by chemical vapor deposition. *Applied Physics A: Materials Science and Processing*, 74(3), 397–402. <https://doi.org/10.1007/s003390201284>
- Lim, X.-X., Low, S.-C., & Oh, W.-D. (2023). A critical review of heterogeneous catalyst design for carbon nanotubes synthesis: Functionalities, performances, and prospects. *Fuel Processing Technology*, 241, 107624. <https://doi.org/10.1016/j.fuproc.2022.107624>
- Liu, Y., Zhai, Y., Li, S., Liu, X., Liu, X., Wang, B., Qiu, Z., & Li, C. (2020). Production of bio-oil with low oxygen and nitrogen contents by combined hydrothermal pretreatment and pyrolysis of sewage sludge. *Energy*, 203, 117829. <https://doi.org/10.1016/j.energy.2020.117829>
- Lobiak, E. V., Kuznetsova, V. R., Flahaut, E., Okotrub, A. V., & Bulusheva, L. G. (2020). Effect of Co-Mo catalyst preparation and CH₄/H₂ flow on carbon nanotube synthesis. *Fullerenes Nanotubes and Carbon Nanostructures*, 28(9), 707–715. <https://doi.org/10.1080/1536383X.2020.1749051>
- Lv, X., Zhang, T., Luo, Y., Zhang, Y., Wang, Y., & Zhang, G. (2020). Study on carbon nanotubes and activated carbon hybrids by pyrolysis of coal. *Journal of Analytical and Applied Pyrolysis*, 146, 104717. <https://doi.org/10.1016/j.jaap.2019.104717>
- Makgabutlane, B., Nthunya, L. N., Maubane-Nkadimeng, M. S., & Mhlanga, S. D. (2021). Green synthesis of carbon nanotubes to address the water-energy-food nexus: A critical review. *Journal of Environmental Chemical Engineering*, 9(1), 104736. <https://doi.org/10.1016/j.jece.2020.104736>
- Manawi, Y. M., Ihsanullah, Samara, A., Al-Ansari, T., & Atieh, M. A. (2018). A review of carbon nanomaterials' synthesis via the chemical vapor deposition (CVD) method. *Materials*, 11(5). <https://doi.org/10.3390/ma11050822>

- Mazumder, S., Sarkar, N., Park, J. G., & Kim, I. J. (2015). A novel processing technique for CNTs growth on Co-supported molecular sieve coated porous ceramics. *Materials Letters*, *161*, 212–215. <https://doi.org/10.1016/j.matlet.2015.08.097>
- Ming, H., Peiling, D., Yunlong, Z., Jing, G., & Xiaoxue, R. (2016). Effect of Reaction Temperature on Carbon Yield and Morphology of CNTs on Copper Loaded Nickel Nanoparticles, *Journal of Nanomaterials*, *2016*, 106845. <https://doi.org/10.1155/2016/8106845>
- Mohammadian, N., Ghoreishi, S. M., Hafeziyeh, S., Saeidi, S., & Dionysiou, D. D. (2018). Optimization of synthesis conditions of carbon nanotubes via ultrasonic-assisted floating catalyst deposition using response surface methodology. *Nanomaterials*, *8*(5), 1–14. <https://doi.org/10.3390/nano8050316>
- Mohd Ghazali, M. S., Md Zaini, M. S., Arshad, M., & Syed-Hassan, S. S. A. (2024). Co-production of biochar and carbon nanotube from sewage sludge in a two-stage process coupling pyrolysis and catalytic chemical vapor deposition. *Waste Disposal & Sustainable Energy*, *6*, 323–334. <https://doi.org/10.1007/s42768-024-00194-2>
- Naqvi, S. R., Tariq, R., Hameed, Z., Ali, I., Naqvi, M., Chen, W.-H., Ceylan, S., Rashid, H., Ahmad, J., & Taqvi, S. A. (2019). Pyrolysis of high ash sewage sludge: Kinetics and thermodynamic analysis using Coats-Redfern method. *Renewable Energy*, *131*, 854–860. <https://doi.org/10.1016/j.renene.2018.07.094>
- Ping, W., & Wang, J. (2016). Comprehensive characterisation of sewage sludge for thermochemical conversion processes – Based on Singapore survey. *Waste Management*, *54*, 131–142. <https://doi.org/10.1016/j.wasman.2016.04.038>
- Prasek, J., Drbohlavova, J., Chomoucka, J., Hubalek, J., Jasek, O., Adam, V., & Kizek, R. (2011). Methods for carbon nanotubes synthesis - Review. *Journal of Materials Chemistry*, *21*(40), 15872–15884. <https://doi.org/10.1039/c1jm12254a>
- Roslan, S. Z., Zainudin, S. F., Aris, A. M., Chin, K. B., Musa, M., Rafizan, A., Daud, M., Shatir, S., & Hassan, A. S. (2023). Hydrothermal Carbonization of Sewage Sludge into Solid Biofuel : Influences of Process Conditions on the Energetic Properties of Hydrochar. *Energies*, *16*, 2483. <https://doi.org/10.3390/en16052483>
- Shah, K. A., & Tali, B. A. (2016). Synthesis of carbon nanotubes by catalytic chemical vapour deposition: A review on carbon sources, catalysts and substrates. *Materials Science in Semiconductor Processing*, *41*, 67–82. <https://doi.org/10.1016/j.mssp.2015.08.013>
- Shahbeig, H., & Nosrati, M. (2020). Pyrolysis of municipal sewage sludge for bioenergy production: Thermo-kinetic studies, evolved gas analysis, and techno- socio-economic assessment. *Renewable and Sustainable Energy Reviews*, *119*, 109567. <https://doi.org/10.1016/j.rser.2019.109567>
- Paul, S., Mondal, S., Saha, A., & Roy, S. (2023). Fundamentals and functionalization of CNTs and other carbon nanomaterials. *Micro and Nano Technologies*, *77*–90. <https://doi.org/10.1016/B978-0-12-824366-4.00008-X>
- Syed-Hassan, S. S. A., Wang, Y., Hu, S., Su, S., & Xiang, J. (2017). Thermochemical processing of sewage sludge to energy and fuel: Fundamentals, challenges and considerations. *Renewable and Sustainable Energy Reviews*, *80*, 888–913. <https://doi.org/10.1016/j.rser.2017.05.262>
- Wang, C., Chang, J., Amatoso, T., Guo, Y., Lin, F., & Yen, Y. (2018). Carbon Nanotubes Grown Using Solid Polymer Chemical Vapor Deposition in a Fluidized Bed Reactor with Iron(III) Nitrate, Iron(III) Chloride and Nickel(II) Chloride Catalysts. *Inventions*, *3*(1), 18. <https://doi.org/10.3390/inventions3010018>

- Wang, J., Shen, B., Lan, M., Kang, D., & Wu, C. (2020). Carbon nanotubes (CNTs) production from catalytic pyrolysis of waste plastics: The influence of catalyst and reaction pressure. *Catalysis Today*, 351, 50–57. <https://doi.org/10.1016/j.cattod.2019.01.058>
- Yu, Z., Chen, D., Tøtdal, B., & Holmen, A. (2005). Effect of catalyst preparation on the carbon nanotube growth rate. *Catalysis Today*, 100(3–4), 261–267. <https://doi.org/10.1016/j.cattod.2004.09.060>
- Zaini, M. S. M., & Jalil, M. J. (2021). A Preliminary Study of the Sustainability of Oil Palm Biomass as Feedstock: Performance and Challenges of the Gasification Technology in Malaysia. *Kem. Ind.*, 70(11–12), 717–728. <https://doi.org/10.15255/kui.2020.077>
- Zhang, S., Qian, L., Zhao, Q., Wang, Z., Lin, D., & Liu, W. (2020). Carbon nanotube : Controlled synthesis determines its future. *Sci. China Mater.* 63, 16–34. <https://doi.org/10.1007/s40843-019-9581-4>
- Zhang, Y. S., Zhu, H. L., Yao, D., Williams, P. T., Wu, C., Xu, D., Hu, Q., Manos, G., Yu, L., Zhao, M., Shearing, P. R., & Brett, D. J. L. (2021). Thermo-chemical conversion of carbonaceous wastes for CNT and hydrogen production: A review. *Sustainable Energy and Fuels*, 5(17), 4173–4208. <https://doi.org/10.1039/d1se00619c>